

SYNTHESIS OF AlPO₄ AND KINETICS OF THERMAL DECOMPOSITION OF AlPO₄·H₂O-H4 PRECURSOR

B. Boonchom^{1,2}, S. Youngme¹, T. Srithanratana¹ and C. Danvirutai^{1*}

¹Department of Chemistry, Faculty of Science, Khon Kaen University, Khon Kaen 40002, Thailand

²King Mongkut's Institute of Technology Ladkrabang Chumphon Campus, 17/1 M. 6 Pha Thiew District, Chumphon 86160, Thailand

The thermal decomposition of aluminum phosphate monohydrate AlPO₄·H₂O-H4 was investigated in air using TG-DTG/DTA. The AlPO₄·H₂O-H4 decomposes in one step and final decomposition product (AlPO₄) was studied by X-ray powder diffraction, FTIR and FT-Raman spectroscopy. The activation energies of dehydration reaction of AlPO₄·H₂O-H4 were calculated through the isoconversional methods of Ozawa and Kissinger–Akahira–Sunose (KAS), and the possible conversion functions have been estimated through the comparative methods. The activation energy calculated for the decomposition of AlPO₄·H₂O-H4 by different methods and techniques were found to be consistent. The kinetic model that better described the reaction of dehydration for AlPO₄·H₂O-H4 was the F_n model as simple *n*-order reaction and the corresponding function is $f(\alpha)=(1-\alpha)^{2.75}$ and $g(\alpha)=-[1-(1-\alpha)^{-1.75}]/(1.75)$.

Keywords: AlPO₄·H₂O-H4, aluminum phosphate, non-isothermal dehydration kinetics

Introduction

Thermal treatment of inorganic phosphate substances has a great synthetic potential as it may turn simple compounds into advanced materials, such as ceramics, catalysts and glasses. The mechanism and kinetics studies of solid-state reactions are needed in order to take advantage of this potential [1–3]. In this respect, amorphous AlPO₄ has attracted the interest of many researchers due to the realization that AlPO₄ is completely iso-structural with silica and exhibits parallel polymorphic transformation [4]. However, the reasons of high catalytic activity remain a point of contention. Thus, in the last few years many works have undertaken a series of research studies on the synthesis, characterization and catalytic activity of different AlPO₄ [4]. The discovery of aluminum phosphate molecular sieves [5] generated a flurry of activity in molecular sieve synthesis. As new structural types began to emerge, there was renewed interest in family of aluminum phosphate referred to as the H series discovered by D'Yoire four decades earlier [6]. Structural characterization of the aluminum phosphates H1 through H4, which were generally all thought to be molecular sieves [5], is incomplete. The aluminum phosphate AlPO₄·H₂O-H4 was first reported in 1961 [6], however, the crystal structure was determined only recently [5]. AlPO₄·H₂O-H4 is not a molecular sieve but rather an interesting condensed aluminum phosphate phase having half of the aluminum atoms four coordi-

nates and the other half six coordinates. The key factor in obtaining AlPO₄ with different properties has been the use of different preparative methods. In the literature, AlPO₄ have been prepared with thermal decomposition of AlPO₄·2H₂O, AlPO₄·H₂O-H1-3 and AlPO₄-21 precursors [7–10].

In the present study, the formation of AlPO₄ from AlPO₄·H₂O-H4 was followed using differential thermal analysis-thermogravimetry (TG-DTG/DTA), X-ray powder diffraction (XRD), Fourier transform-infrared (FTIR) and Fourier transform-Raman spectroscopy (FT-Raman). The kinetics analysis of the non-isothermal results for the aluminum phosphate decomposition steps were carried out using the isoconversional methods of Ozawa [11] and Kissinger-Akahira-Sunose (KAS) [12] and the possible conversion functions had been estimated through the comparative methods. In the literature there is no report on the thermal decomposition kinetics of AlPO₄·H₂O-H4. So the aim of this work is to investigate the kinetic parameters of dehydration of AlPO₄·H₂O-H4.

Experimental

AlPO₄·H₂O-H4 was prepared according to the previous methods [5, 13] by stirring 1.096 g of Al₂O₃, 2.27 mL of 86.4 mass/mass% H₃PO₄ and 9.9 mL of deionized water for 2 h followed by the addition of 0.77 mL of

* Author for correspondence: chanai@kku.ac.th

tripropylamine (TPA) and further stirring by 45 min. The gel was aged at room temperature for 1 h and then transferred to a Teflon-lined Parr reactor at 150°C under static conditions for 25 h. The white powders were isolated by filtration, washed with deionized water and dried at 70°C overnight.

Thermal analysis measurements (thermogravimetry, (TG), differential thermogravimetry, (DTG), and differential thermal analysis, (DTA)) were carried out by a Pyris Diamond Perkin-Elmer apparatus by increasing temperature from 50 to 400°C with calcined $\alpha\text{-Al}_2\text{O}_3$ powder as the standard reference. The experiments were performed in static air, at heating rates of 5, 10, 15 and 20°C min⁻¹. The sample mass was kept 6.0–10.0 mg into alumina crucible without pressing.

The structure and crystalline size of the prepared product and the calcined sample were studied by X-ray powder diffraction using a D8 Advanced powder diffractometer (Bruker AXS, Karlsruhe, Germany) with CuK α radiation ($\lambda=0.15406$ Å). The Scherrer method was used to evaluate the crystalline size.

The room temperature FTIR spectra were recorded in the range of 4000–370 cm⁻¹ with 8 scans on a Perkin-Elmer Spectrum GX FT-IR/FT-Raman spectrometer with the resolution of 4 cm⁻¹ using KBr pellets (KBr, Jasco, spectroscopy grade). The FT-Raman spectra were recorded with spectrum 2000R NIR FT-Raman system in a Perkin-Elmer Spectrum GX model equipped with a HeNe laser (1064 nm). The laser power about 500 mW was used for excitation in the range between 4000–100 cm⁻¹ with 32 scans.

Results and discussion

Thermal analysis

TG curves of the thermal decomposition of AlPO₄·H₂O-H4 at four heating rates are shown in

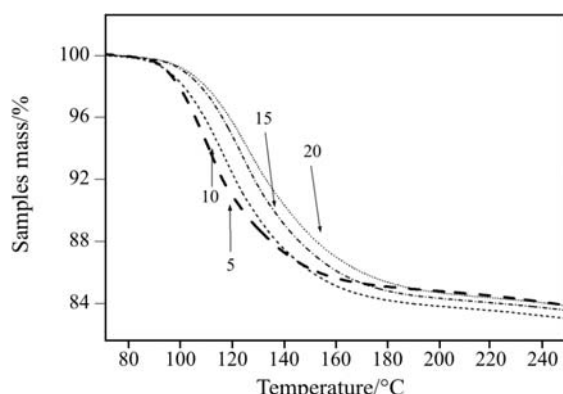


Fig. 1 TG curves of AlPO₄·H₂O-H4 in air at four heating rates (5, 10, 15 and 20°C min⁻¹)

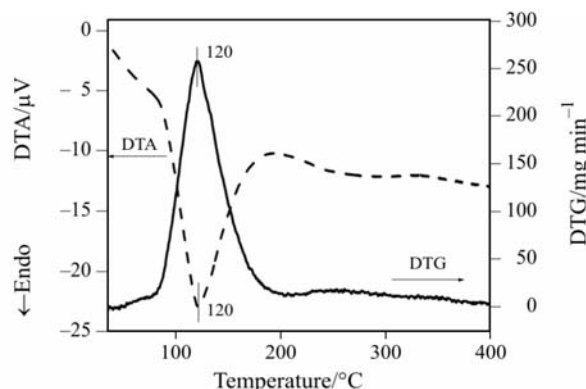


Fig. 2 DTG-DTA curves of AlPO₄·H₂O-H4 at heating rate of 10°C min⁻¹ in air

Fig. 1. All curves are approximately in the same shape and indicated that the mass loss is independent of the heating rate. DTG-DTA curves of AlPO₄·H₂O-H4 at the heating rate of 10°C min⁻¹ in air are shown in Fig. 2. The TG curve shows that the thermal decomposition at temperatures below 200°C occurs through one well-defined step. The peak in the DTG curve closely corresponds to the mass loss observed on the TG trace. The mass retained is about 85% for all heating rates, compatible with the value expected for the formation of AlPO₄, which is verified by XRD measurement. The mass loss in the range of 50–200°C depends on the heating rate: the mass loss increases with the decreasing of the heating rate. The mass loss at all four heating rates is between 14.58 and 16.48% much larger than the mass loss of the release of one water molecule [5]. The water eliminated at 200°C and below can be considered as the water of crystallization. In the DTA curve, the corresponding peak at 120°C is observed. An endothermic effect over the temperature region is shown in the DTA curve at 120°C. The overall reaction is:



The temperature at which theoretical mass loss is achieved and can be also determined from the TG curves and considered to be the minimum temperatures needed for the calcinations process. Thus, AlPO₄·H₂O-H4 sample was calcined at 200°C for 2 h in the furnace.

X-ray powder diffraction

The XRD patterns of aluminum phosphate AlPO₄·H₂O-H4 and its dehydration product (AlPO₄) are shown in Fig. 3. All detectable peaks are indexed as the AlPO₄·H₂O-H4 and AlPO₄ with structure in standard data as PDF #821454 and PDF #511674, respectively. These results indicated that both crystal structures are in monoclinic system with space group

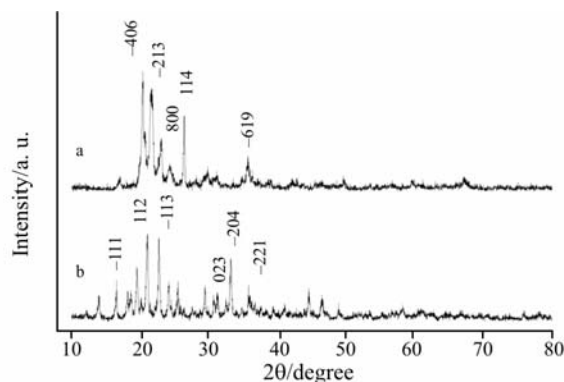


Fig. 3 The XRD patterns of a – AlPO₄·H₂O-H4 and b – its dehydration product (AlPO₄)

C2/c ($Z=8$) for AlPO₄·H₂O-H4 and P_c ($Z=2$) for AlPO₄. The average crystallite size of 67 ± 25 nm for AlPO₄·H₂O-H4 sample was calculated from X-ray line broadening of the reflections of (-111), (112), (-113) and (-221), using Scherrer equation (i.e. $D=0.89\lambda/\beta\cos\theta$), where λ is the wavelength of X-ray radiation, θ is the diffraction angle and β is the full width at half maximum (FWHM)) [14–16]. Similarly, the average crystallite size of 55 ± 19 nm for calcined sample (AlPO₄) was calculated from X-ray line broadening of the reflections of (-406), (-213), (114) and (-619). The lattice parameters calculated from the XRD spectra are $a=7.13(5)$, $b=7.10(6)$, $c=12.80(2)$ Å for AlPO₄·H₂O-H4 and $a=37.02(9)$, $b=5.00(7)$, $c=25.97(1)$ Å for AlPO₄. The lattice parameters of AlPO₄·H₂O-H4 and of calcined sample (AlPO₄) are close to those of the standard data as PDF #821454 and PDF #511674, respectively. The particle sizes and lattice parameters are also tabulated in Table 1.

Vibrational spectroscopy

FTIR and FT-Raman spectra of AlPO₄·H₂O-H4 and its dehydration product (AlPO₄) are shown in Figs 4 and 5. Vibrational bands are identified in relation to the crystal structure in terms of the fundamental vibrating units namely PO₄³⁻, H₂O, AlO₄, AlO₆ for AlPO₄·H₂O-H4 and PO₄³⁻, AlO₆ for AlPO₄ [17–19]. FTIR and FT-Raman spectra of PO₄³⁻ in AlPO₄·H₂O-H4 show symmetric stretching mode (v_1)

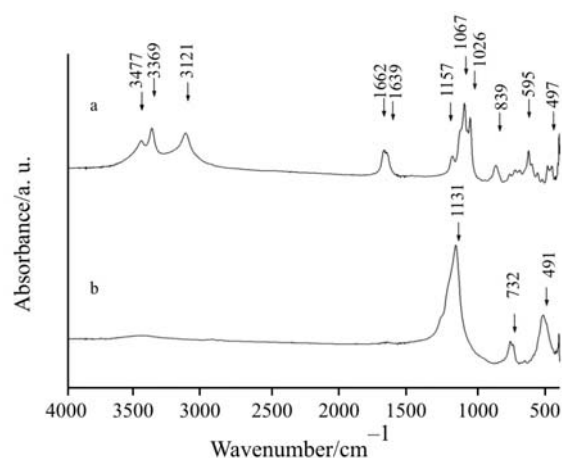


Fig. 4 FT-IR spectra of a – AlPO₄·H₂O-H4 and b – its dehydration product (AlPO₄)

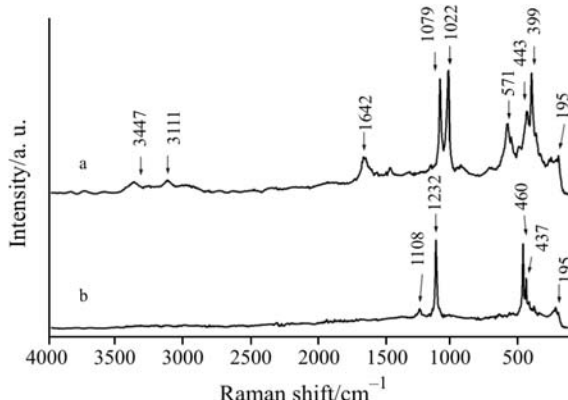


Fig. 5 FT-Raman spectra of a – AlPO₄·H₂O-H4 and b – its dehydration product (AlPO₄)

at 1022 (IR), 1017 (R) cm⁻¹, the antisymmetric stretching mode (v_3) at 1153 (IR), 1089 (IR), 1067 (IR), 1111 (R) and 1074 (R) cm⁻¹, the symmetric bending mode (v_2) at 411 (IR), 391 (R) cm⁻¹, and the v_4 mode at 497 (IR), 458 (IR), 422 (IR), 433 (R) cm⁻¹. The observed multiple characteristic phosphate bands provide an indication of symmetry reduction of the PO₄³⁻ units and two non-equivalent phosphates in the structure [20]. The observed bands at 1600–1660 and 3000–3500 cm⁻¹ region are attributed to the water bending and stretching vibrations. Finally, the bands at 694 and 526 cm⁻¹ are assigned to the water liberations.

Table 1 Average particle sizes and lattice parameters of AlPO₄·H₂O and AlPO₄ calculated from XRD data

Compounds	Work	Lattice parameters				Average particle sizes/nm
		$a/\text{\AA}$	$b/\text{\AA}$	$c/\text{\AA}$	$\beta/^\circ$	
AlPO ₄ ·H ₂ O-H4	PDF #511674	7.14	7.09	12.74	99.10	–
	This work	7.13(5)	7.10(6)	12.80(2)	99.04(0)	67 ± 25
	DIF. (This work-PDF)	-0.01	+0.01	+0.06	-0.06	
AlPO ₄	PDF #821454	37.39	5.05	26.22	117.84	–
	This work	37.02(9)	5.00(7)	25.97(1)	117.67(8)	55 ± 19
	DIF. (This work-PDF)	-0.36	-0.05	-0.25	-0.16	

These water bands are disappeared in FTIR and FT-Raman of its dehydration product (AlPO_4). Additionally, FTIR and FT-Raman spectra of PO_4^{3-} in AlPO_4 show symmetric stretching mode (v_1) at 1108 (R) cm^{-1} , the antisymmetric stretching mode (v_3) at $1232\text{ (R) and }1131\text{ (IR) cm}^{-1}$, the symmetric bending mode (v_2) at $460\text{ (R), }437\text{ (R) cm}^{-1}$ and the v_4 mode at 491 (IR) cm^{-1} . The XRD data along with FTIR and FT-Raman spectra confirm the calcined $\text{AlPO}_4 \cdot \text{H}_2\text{O-H4}$ at 200°C for 2 h show that transformation of $\text{AlPO}_4 \cdot \text{H}_2\text{O-H4}$ leads to AlPO_4 .

Kinetics studies

Calculation of the activation energy

Dehydration of crystal hydrates is a solid-state process of the type [21–24]: A (solid) \rightarrow B (solid) + C (gas). The kinetics of such reactions is described by various equations taking into account the special features of their mechanisms. This is a model-free method, which involves measuring the temperatures corresponding to fixed values of α (extent of conversion) from experiments at different heating rates (β). The activation energy (E_a) can be calculated according to the isoconversional methods. In kinetic study of $\text{AlPO}_4 \cdot \text{H}_2\text{O-H4}$, Ozawa [11] and KAS [12] equations were used to determine the activation energy of the dehydration reaction.

The equations used for E_a calculation are:

- Ozawa equation:

$$\log\beta = \log\left(\frac{AE_a}{Rg(\alpha)}\right) - 2.315 - 0.4567\left(\frac{E_a}{RT}\right) \quad (2)$$

- KAS equation:

$$\ln\left(\frac{\beta}{T^2}\right) = \ln\left(\frac{AE_a}{Rg(\alpha)}\right) - \left(\frac{E_a}{RT}\right) \quad (3)$$

where A (the pre-exponential factor) and E (the activation energy) are the Arrhenius parameters and R is the gas constant ($8.314\text{ J mol}^{-1}\text{K}^{-1}$). The Arrhenius parameters, together with the reaction model, are sometimes called the kinetic triplet. $g(\alpha) = \int_0^\alpha \frac{d\alpha}{f(\alpha)}$ is

the integral form of the $f(\alpha)$, which is the reaction model that depends on the reaction mechanism.

At the constant condition of other parameters, the TG curves for dehydration of $\text{AlPO}_4 \cdot \text{H}_2\text{O-H4}$ in air at various heating rates (5, 10, 15 and $20^\circ\text{C min}^{-1}$) are shown in Fig. 1. According to isoconversional method, the basic data of α and T collected from Fig. 1 are illustrated in Table 2. According to the above-mentioned equations, the plots of $\log\beta$ vs. $1000/T$ (Ozawa) and $\log\beta/T^2$ vs. $1000/T$ (KAS) cor-

Table 2 $\alpha-T$ data at different heating rates, β ($^\circ\text{C min}^{-1}$), for dehydration of $\text{AlPO}_4 \cdot \text{H}_2\text{O-H4}$

α	Temperature/K			
	$\beta=5$	$\beta=10$	$\beta=15$	$\beta=20$
0.2	380.92	384.64	388.76	390.83
0.3	384.31	388.87	393.58	396.25
0.4	387.64	393.09	398.07	401.27
0.5	391.71	397.62	402.64	406.32
0.6	397.25	403.16	408.38	412.59
0.7	403.89	409.76	415.05	419.75
0.8	412.45	418.61	423.89	428.62
0.9	425.33	431.88	436.78	441.78

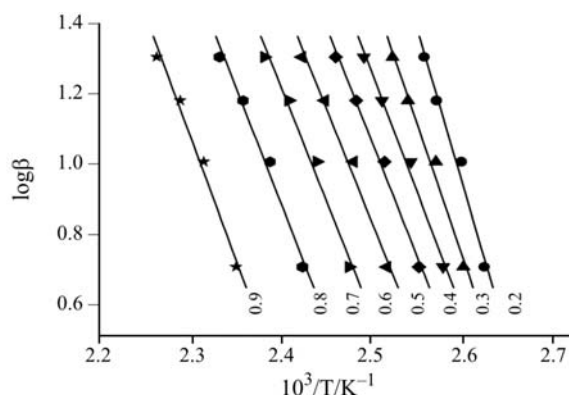
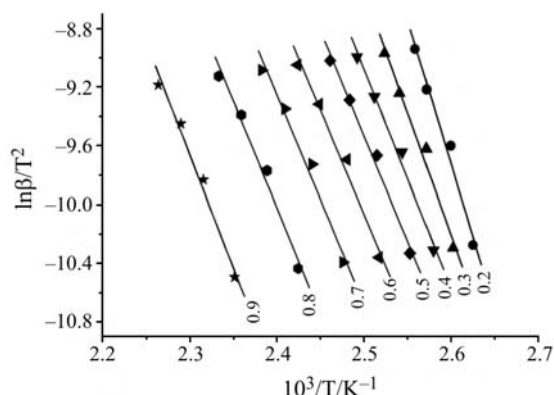
Table 3 Activation energies (E_a) vs. correlation coefficient (r^2) calculated by Ozawa and KAS methods for the dehydration of $\text{AlPO}_4 \cdot \text{H}_2\text{O-H4}$

α	Ozawa method		KAS method	
	$E_a/\text{kJ mol}^{-1}$	r^2	$E_a/\text{kJ mol}^{-1}$	r^2
0.2	159.10	0.991	160.89	0.990
0.3	136.33	0.993	136.88	0.992
0.4	123.39	0.995	123.20	0.994
0.5	118.73	0.996	118.23	0.995
0.6	116.57	0.993	115.85	0.992
0.7	116.72	0.990	115.90	0.989
0.8	119.74	0.992	118.93	0.991
0.9	126.20	0.993	125.51	0.992
Average	127.10 \pm 13	0.992	126.92 \pm 14	0.991

responding to different conversions α can be obtained by a linear regression of least-square method, respectively. The Ozawa and KAS analysis results of four TG measurements below 200°C are presented in Figs 6 and 7, respectively. The activation energies E_a can be calculated from the slopes of the straight lines with better linear correlation coefficient (r^2). The slopes change depending on the degree of conversion (α) for the dehydration reaction of $\text{AlPO}_4 \cdot \text{H}_2\text{O-H4}$. The activation energies are calculated at heating rates of 5, 10, 15, and $20^\circ\text{C min}^{-1}$ via the Ozawa and KAS methods in the α range of 0.2 to 0.9. The activation energies calculated by Ozawa and KAS methods are close to each other, which are shown in Table 3, so the results are credible. The activation energy values calculated by the KAS method are close to those obtained by Ozawa method. The activation energies change little with α , so we draw a conclusion that the dehydration reaction of $\text{AlPO}_4 \cdot \text{H}_2\text{O-H4}$ would be a single kinetic mechanism, corresponding to an endothermic peak at 120°C in DTA curve.

Table 4 Kinetics parameters obtained from the differential method and integral method at different heating rates ($\beta=5, 10, 15, 20^{\circ}\text{C min}^{-1}$)

$\beta^{\circ}\text{C min}^{-1}$	Model F _n	Coats–Redfern method			Achar method		
		$E_a/\text{kJ mol}^{-1}$	$\ln A/\text{s}^{-1}$	r^2	$E_a/\text{kJ mol}^{-1}$	$\ln A/\text{s}^{-1}$	r^2
5	F _{2.75}	131.58	32.97	0.996	127.49	38.90	0.994
10	F _{2.75}	128.50	32.15	0.999	133.20	40.65	0.997
15	F _{2.75}	129.68	32.43	0.999	139.69	42.44	0.997
20	F _{2.75}	123.88	30.61	0.999	136.79	41.44	0.996
Average	F _{2.75}	128.41±2.8	32.04±0.8	0.998	134.29±2.8	40.86±1.3	0.996

**Fig. 6** Ozawa analysis of four TG measurements below 200°C**Fig. 7** KAS analysis of four TG measurements below 200°C

Estimation of the conversion function and the pre-exponential factor

For one-step reaction, the estimation of kinetic parameters can be turned into a multiple linear regression problem through the Coats–Redfern [25] and Achar equations [26].

- Coats–Redfern equation:

$$\ln\left(\frac{g(\alpha)}{T^2}\right) = \ln\left(\frac{AE_\alpha}{Rg(\alpha)}\right) - \left(\frac{E_\alpha}{RT}\right) \quad (4)$$

- Achar equation:

$$\ln\left(\frac{1}{f(\alpha)} \frac{d\alpha}{dT}\right) = \ln\left(\frac{AE_\alpha}{Rg(\alpha)}\right) - \left(\frac{E_\alpha}{RT}\right) \quad (5)$$

Hence, $\ln\left(\frac{g(\alpha)}{T^2}\right)$ and $\ln\left(\frac{1}{f(\alpha)} \frac{d\alpha}{dT}\right)$ calculated

for the different α values at the single β value on $1/T$ must give rise to a single master straight line, so the activation energy and the pre-exponential factor can be calculated from the slope and intercept through ordinary least square estimation. The activation energy, pre-exponential factor and the correlation coefficient can be calculated through the equation of the Coats–Redfern and Achar methods combined with 31 conversion functions [21, 27]. Generally speaking, the one with highest correlation coefficient (>0.99) is the best-fit kinetic model. The optimized values from the Coats–Redfern and Achar methods are the data of activation energy and $\ln A$, which were calculated with the best equation. Experimental results are shown in Table 4. According to Table 4, it was seen that the values calculated by Ozawa and KAS methods were close to the optimized values from the Coats–Redfern and Achar methods, and the respective correlation coefficients are preferable.

From the above analysis, we can draw a conclusion that the obtained possible conversion function is F_n model for the dehydration of AlPO₄·H₂O-H₄, and the corresponding function is $f(\alpha)=(1-\alpha)^n$ and $g(\alpha)=[1-(1-\alpha)^{1-n}]/(1-n)$. The correlated kinetic parameters are $E_a=128.41\pm2.8 \text{ kJ mol}^{-1}$ (Coats–Redfern) and $134.29\pm2.8 \text{ kJ mol}^{-1}$ (Achar), $\ln A=32.04\pm0.8 \text{ s}^{-1}$ (Coats–Redfern) and $40.86\pm1.3 \text{ s}^{-1}$ (Achar), $n=1.75$ (Coats–Redfern and Achar), respectively.

Conclusions

AlPO₄·H₂O-H₄ decomposes in one step by starting after 100°C and the final product is AlPO₄. The dehydration of AlPO₄·H₂O-H₄ is important for its further treatments. The final product is confirmed by XRD data and FTIR and FT-Raman measurements. Kinetic analysis from non-isothermal TG applying model-fitting method results a single value of E on the different α which can be assigned to a simple reaction. The activation energy calculated for the decomposition of

$\text{AlPO}_4 \cdot \text{H}_2\text{O-H4}$ by different methods and techniques were found to be consistent. This indicates that the activation energy of decomposition is independent on process and the nature of non-isothermal methods as well as TG. The kinetic model that better described the reaction of dehydration for $\text{AlPO}_4 \cdot \text{H}_2\text{O-H4}$ was the F_n model as simple n -order reaction. The corresponding function is $f(\alpha) = (1-\alpha)^{2.75}$ and $g(\alpha) = -[1-(1-\alpha)^{-1.75}]/(1.75)$ and were reported for the first time.

Acknowledgements

The authors would like to thank the Chemistry and Physics Departments, Khon Kaen University for providing research facilities. This work is financially supported by King Mongkut's Institute of Technology Ladkrabang (KMITL) and the Center for Innovation in Chemistry: Postgraduate Education and Research Program in Chemistry (PERCH-CIC), The Ministry of Education, Thailand.

References

- 1 J. Hong, G. Guo and K. Zhang, *J. Anal. Appl. Pyrolysis*, 2 (2006) 111.
- 2 V. Logvinenko, *J. Therm. Anal. Cal.*, 60 (2000) 9.
- 3 S. Vyazovkin, *Anal. Chem.*, 74 (2002) 2749.
- 4 F. M. Bautista, J. M. Campelo, A. García, D. Luna, J. M. Marinas, R. A. Quirós and A. A. Romero, *Appl. Catal. A*, 243 (2003) 93, and references therein.
- 5 D. M. Poojary, K. J. Balkus, S. J. Riley, B. E. Gnade and A. Clearfield, *Micropor. Mater.*, 2 (1994) 245 and references therein.
- 6 F. D'Yvoire, *Bull. Soc. Chim. Fr.*, (1961) 1762.
- 7 K. Kunii, K. Narahara and S. Yamanaka, *Macropor. Mesopor. Mater.*, 52 (2000) 159.
- 8 S. T. Wilson, B. M. Lok, C. A. Messina, T. R. Cannan and E. M. Flanigan, *J. Am. Chem. Soc.*, 104 (1982) 1146.
- 9 N. Venkatathri, *Bull. Mater. Sci.*, 26 (2003) 279.
- 10 D. Stojakovic, N. Rajic, S. Sajic, N. Z. Logas and V. Kaucic, *J. Therm. Anal. Cal.*, 87 (2007) 339.
- 11 T. Ozawa, *Bull. Chem. Soc. Jpn.*, 38 (1965) 1881.
- 12 H. E. Kissinger, *J. Anal. Chem.*, 29 (1957) 1702.
- 13 K. J. Balkus Jr., L. J. Sottile, S. J. Riley and B. E. Gnade, *Thin Solid Films*, 260 (1995) 4.
- 14 B. D. Cullity, *Elements of X-ray Diffraction*, 2nd Ed., Addison-Wesley Publishing, 1977.
- 15 G. K. Williamson and W. H. Hall, *Acta Metall.*, (January) (1953) 22.
- 16 M. Zakeri, R. Yazdani-Rad, M. H. Enayati and M. R. Rahimipour, *J. Alloys Compd.*, 403 (2005) 258.
- 17 P. Tarte, *Spectrochim. Acta*, 23A (1967) 2127.
- 18 R. L. Frost and M. L. Weier, *J. Mol. Struct.*, 697 (2004) 207.
- 19 D. K. Breitinger, J. Mohr, D. Colognesi, S. F. Parker, H. Schukow and R. G. Schwab, *J. Mol. Struct.*, 563–564 (2001) 377.
- 20 R. L. Frost and M. L. Weier, W. N. Martens, D. A. Henry and S. J. Mills, *Spectrochim. Acta*, 62A (2005) 181 and references therein.
- 21 T. V. Lyubomir, M. M. Nikolova and G. G. Gospodinov, *J. Solid State Chem.*, 177 (2004) 2663.
- 22 S. Vyazovkin, *Int. J. Chem. Kinet.*, 28 (1996) 95.
- 23 S. Vyazovkin, *Thermochim. Acta*, 355 (1996) 155.
- 24 K. Zhang, J. Hong, G. Cao, D. Zhan, Y. Tao and C. Cong, *Thermochim. Acta*, 437 (2005) 145.
- 25 A. W. Coats and J. P. Redfern, *Nature*, 20 (1964) 68.
- 26 B. N. Achar, *Proc. Int. Clay Conf.*, 1 (1966) 67.
- 27 X. Gao and D. Dollimore, *Thermochim. Acta*, 215 (1993) 47.

Received: February 27, 2007

Accepted: April 24, 2007

DOI: 10.1007/s10973-007-8420-1